Journal of Applied Pharmaceutical Research
Volume 14 Issue 4, Year of Publication 2026, Page 79 – 96
DOI: https://doi.org/10.69857/joapr.v14i4.2247

Check for updates

Research Article

JOURNAL OF APPLIED PHARMACEUTICAL RESEARCH | JOAPR
www.japtronline.com ***ISSN: 2348 – 0335***

QUALITY BY DESIGN BASED OPTIMIZATION AND PHYSICOCHEMICAL CHARACTERIZATION OF FLUCYTOSINE NANOEMULSION

Rajat Srivastava*, Ajay Kumar Singh Rawat

Article Information
Received: 31st January 2026
Revised: 10th May 2026
Accepted: 23rd June 2026
Published: 31st July 2026

Keywords
Pathogenic fungi, Nanoemulsion, Box-Behnken design (BBD), Antifungal drugs, Bioavailability.

ABSTRACT
Background: The rise of pathogenic fungi capable of infecting people is a major public health problem. Flucytosine is an effective antifungal agent, but its clinical use is constrained by rapid clearance and dose-related adverse effects. Nanoemulsion-based systems offer a promising strategy for drug delivery and therapeutic performance. The objective of this work was to develop and optimize a flucytosine-loaded nanoemulsion using a Quality by Design (QbD) approach based on the Box-Behnken design, and to evaluate its physicochemical characteristics. **Methodology:** A Box-Behnken design (BBD) was used to optimize formulation factors, including lipid concentration, Smix (surfactant-to-cosurfactant) ratio, and homogenization time, using high-speed homogenization. The impacts on particle size, polydispersity index, and entrapment efficiency (EE) were investigated. UV-visible spectroscopy, Fourier-transform infrared spectroscopy (FTIR), and X-ray diffraction (XRD) were used to assess the compatibility and stability of the improved formulation (F11) with the chosen excipients. **Results and Discussion:** The optimized formulation (F11) had a particle size of 318.18 nm and a PDI of 0.136, a zeta potential of -22.2 mV, and high entrapment efficiency (96.36%), indicating good stability and uniformity. Preformulation and compatibility studies confirmed the absence of drug-excipient interactions. Statistical analysis demonstrated that formulation variables significantly influenced critical quality attributes. **Conclusion:** The study demonstrates that QbD-driven optimization can successfully develop a stable and efficient flucytosine nanoemulsion with enhanced drug-loading capacity and potential to improve antifungal therapy. However, further studies, including in vitro drug release, in vivo evaluation, long-term stability, and clinical validation, are required to confirm its performance in drug delivery applications.

INTRODUCTION

The emergence of pathogenic fungi capable of infecting humans is a significant public health concern [1]. Fungal diseases such as blastomycosis and histoplasmosis are commonly treated with several medications available on the market, including topical and oral options. However, oral medications have low

*Maharishi School of Pharmaceutical Sciences, Maharishi University of Information Technology, Lucknow, Uttar Pradesh, 226013, India.

***For Correspondence:** **rajatb.srivastava@gmail.com**

bioavailability, which reduces their effectiveness [2]. Flucytosine, an antifungal agent with potent activity against *Cryptococcus* and *Candida* species, has been a pivotal component in the treatment of severe fungal infections for decades [3]. Despite its efficacy, access to flucytosine remains limited in many regions, hindering its widespread use in combating invasive fungal diseases [4]. The synergistic effect of flucytosine in combination therapy, particularly with amphotericin B, has shown promising results in improving survival rates in *cryptococcal meningitis* and reducing mortality in *Candida meningitis*, emphasizing its crucial role in managing these life-threatening infections [5]. However, challenges such as the emergence of resistance during monotherapy for certain fungal infections underscore the importance of further research and efforts to enhance access to flucytosine, especially in low-income countries, to mitigate the impact of invasive fungal diseases [6].

Flucytosine, an antifungal agent effective against *Cryptococcus* and *Candida* species, exerts its action by inhibiting fungal DNA and RNA synthesis [7]. This mechanism hinders nucleic acid metabolism, impairs protein synthesis, and ultimately leads to fungal cell death. Due to its high water solubility, flucytosine can readily enter several parts of the body, including the eye, urinary tract, central nervous system, and cardiac vegetations. This ability enhances its effectiveness in treating fungal infections. When flucytosine is co-administered with amphotericin B, it demonstrates early fungicidal efficacy against Cryptococcus species, leading to improved survival in cryptococcal meningitis [8]. The synergistic effect of flucytosine with amphotericin B has been particularly beneficial in reducing mortality in Candida meningitis and neonatal candidiasis, underscoring its importance in the management of severe fungal infections [9]. After being absorbed by susceptible fungal cells, flucytosine is converted into 5-fluorouracil (5-FU), which subsequently suppresses the synthesis of fungal RNA and DNA. Following oral administration, flucytosine is well absorbed, efficiently penetrates tissues, and is primarily eliminated by the kidneys [3].

Despite flucytosine's high water solubility and efficient absorption, its therapeutic application is limited by rapid systemic clearance and dose-dependent toxicity, driven by elevated peak plasma concentrations and renal excretion. Nanoemulsion-based delivery technologies provide benefits that extend beyond mere solubility augmentation. Integrating flucytosine into a nanoemulsion facilitates controlled, prolonged drug release, thereby reducing plasma concentration fluctuations and minimizing peak-associated side effects. Nanoemulsions can enhance tissue distribution and cellular absorption, potentially improving antifungal activity at the site of infection. Encapsulation within the lipid phase may reduce rapid exposure of free medication to the systemic circulation, thereby reducing renal burden and toxicity. The application of nanoemulsion systems for flucytosine is warranted not for enhancing solubility, but for pharmacokinetic modification, targeted delivery, and an enhanced safety profile. To address these pharmacokinetic and toxicity-related limitations, nanoemulsions (NEs) are being explored as advanced drug delivery systems consisting of two immiscible liquids, usually oil and water, that are stabilized by surface-active agents known as surfactants [10]. Surfactants play a role in emulsification by reducing the likelihood of coalescence through adsorption at the oil-water interface, thereby lowering surface tension. Surfactants aid in the separation or disruption of dispersed phases by forming a film at the oil-water interface, thereby slowing destabilization processes. The selection of surfactants is crucial for developing NEs with precise physicochemical characteristics. Nanoemulsions have droplet sizes ranging from 10 to 1000 nm, which render them kinetically stable but thermodynamically unstable [11]. This instability arises from the increased free energy of the system relative to that of the individual phases [12].

Experimental design is commonly used to optimize nanoparticles due to its benefits, including reducing the number of experiments required, creating mathematical models to evaluate the importance and statistical significance of factor effects, and assessing the interaction effects between factors [13]. Box-Behnken designs are useful tools for optimizing process response surfaces. They originate from a 3-level incomplete factorial design. These designs enable the detection of model fit problems, the generation of sequential designs, and the estimation of quadratic model parameters.

The Box-Behnken design omits combinations in which all elements are simultaneously set to their highest and lowest levels. This hinders testing in extreme conditions, potentially leading to disappointing outcomes. A design matrix including 17 experimental runs was created for the present inquiry. The given design matrix was utilized to generate a quadratic model, expressed by the equation-

$$Y = b_0 + b_1X_1 + b_2X_2 + b_3X_3 + b_{12}X_1X_2 + b_{13}X_1X_3 + b_{23}X_2X_3 + b_{11}X_{12} + b_{22}X_{22} + b_{33}X_{32} \quad -----(1)$$

The observed outcome for each combination of factor levels is denoted by Y. The intercept is denoted as b0, whilst the regression coefficients derived from experimental runs are denoted as b1 to b33. The independent variables are coded as X1, X2, and X3 [14].

The current study employed an experimental design to develop and optimize a flucytosine nanoemulsion to improve drug delivery against fungal infections. However, the evaluation of biological antifungal activity is not included in the current work, which is restricted to formulation development and physicochemical characterization.

MATERIALS AND METHODS

Material

The materials listed below were obtained from the indicated sources without undergoing additional purification. Flucytosine was obtained from BLD Pharma in Hyderabad, India. The remaining chemicals used were of analytical reagent grade.

Methods

PRE-FORMULATION STUDIES

Solubility Studies

Solubility studies were performed to identify suitable oil, surfactant, and cosurfactant for nanoemulsion formulation. Excess flucytosine was added to various oils (castor oil, liquid paraffin), surfactants (Tween 80), and cosurfactants (propylene glycol), then vortexed and shaken for 48 hours at room temperature to achieve equilibrium. The mixtures were centrifuged, and the supernatant was analyzed using UV spectrophotometry at 285 nm. The components exhibiting the highest solubility in flucytosine were selected for further formulation development.

Spectrophotometric analysis of flucytosine

A weighed amount of 100 mg of flucytosine was dissolved in a 100 mL volumetric flask using a diluent of 0.1N HCl (having an exactly known concentration). 10 mL of the stock solution (1000 µg/mL) was transferred to a 100 mL volumetric flask. The sample was dissolved and diluted with diluent (0.1N HCl) until the flask was filled to the mark. The solution was analyzed using a UV-Visible Spectrophotometer (UV-1900i, Shimadzu) over the wavelength range of 200-400 nm. The absorption maximum was identified and compared with the value of 285 nm reported in an official monograph [15].

Fourier Transform Infra-Red Spectroscopy (FT-IR)

The FT-IR technique is highly valuable for identifying both organic and inorganic substances. This tool can be used to evaluate solids, liquids, and gases, as well as to quantify certain components of an unidentified mixture [16]. Fourier Transform Infrared Spectroscopy (FT-IR) determination of flucytosine was performed using PerkinElmer Spectrum IR version 10.7.2. The spectra were produced using the KBr pellet technique, and the reference standard peaks were compared with those obtained. 10 mg of flucytosine was combined with KBr under high compaction pressure. The spectra of the dried mixture of drug and polymers were recorded after baseline adjustment and were obtained by scanning.

Drug - excipients compatibility studies

Any chemical or physical interaction between a drug and its excipients can affect the drug's stability and bioavailability. A physical mixture of drug and excipients (1:1) was prepared and stored under ambient conditions for 4 weeks to evaluate compatibility using FTIR analysis [17].

X-ray diffraction (XRD) study

X-ray diffraction (XRD) is a highly effective and widely used technique in both research and industry. Although XRD is commonly recognized for its ability to qualitatively and quantitatively assess crystalline phases in materials, a meticulous examination of the diffraction patterns can yield a wealth of other information. An XRD analysis was conducted on the pure medication to determine its diffraction pattern [18] quantitatively.

Formulation Development

Selection of Excipients

The selection of formulation components was based on solubility studies, emulsification efficiency, and literature reports. Castor oil and liquid paraffin were selected as the oil phase due to their ability to solubilize the drug and their biocompatibility. Tween 80 was selected as a surfactant owing to its non-ionic nature, high hydrophilic-lipophilic balance (HLB ~15), and ability to stabilize oil-in-water nanoemulsion. Propylene glycol was used as a cosurfactant to enhance interfacial fluidity and improve drug solubilization. These excipients are widely reported in nanoemulsion formulations and provide stability and improved drug-delivery performance.

Preparation of Nanoemulsion as per Experimental Design

Box-Behnken design (BBD) is a well-recognized and commonly adopted method for optimizing nanoemulsion formation. The implementation and interpretation of this method involve experimental techniques, which were compared with other approved methods [19]. Our preliminary study employed statistical methods to identify the independent and dependent variables and their respective limits. A Box-Behnken design (BBD) was implemented to ascertain the [amount of lipid (X1), S_{mix} (X2), and optimal homogenization time (X3)] to facilitate the advancement of nanoemulsion. Table 1 delineates the response parameters, which include particle size (Y1), polydispersity index (PDI) (Y2), and percentage entrapment efficiency (Y3), to assess a broad spectrum of prospective outcomes. The response surface approach is a statistical method that was used to investigate the direct effects of different formulations and/or processing factors on one or more response variables [20]. The most suitable design was selected to optimize the formulation process [21]. The nanoemulsion containing Flucytosine was analyzed using Design-Expert software® version 12.0.3.0 (Stat-Ease Inc., Minneapolis, MN, USA) [22]. The investigation demonstrated that by employing three distinct center locations, it was possible to generate 17 unique formulas. The response surface method commonly uses a complete quadratic equation to estimate the correlation function. Table 2 displays the formulation parameters and the corresponding observations for these dependent variables.

Table 1: Variables in Box-Behnken design.

Factor **Independent variables**	**Levels used**		
	-1	**0**	**+1**
Amount of lipid (%v/v) (X1)	10	12.5	15
S_{mix} (mL) (X2)	1.00	1.25	1.50
Homogenization Time (min) (X3)	15	20	25
Dependent variables	**Constraints**		
Particle size (nm) (Y1)	Minimize		
PDI (Y2)	Minimize		
% Entrapment Efficiency (%) (Y3)	Maximize		

Table 2: Composition and observed responses in Box-Behnken design.

Batch	**Drug**	**Independent variables**			**Dependent variables**		
		Amount of lipid (% v/v) (X1)	**S_{mix} (mL) (X2)**	**Homogenization Time (min) (X3)**	**Particle Size (nm)**	**PDI**	**%EE (%)**
1	10	15	1.25	25	516	0.197	93.81
2	10	12.5	1.25	20	334	0.126	96.51
3	10	15	1.5	20	398	0.143	90.12
4	10	12.5	1.25	20	329	0.132	98.89
5	10	10	1.5	20	757	0.118	91.89
6	10	12.5	1	15	561	0.137	89.45
7	10	15	1	20	583	0.147	93.31
8	10	12.5	1.25	20	343	0.135	97.93
9	10	12.5	1.25	20	347	0.136	96.89
10	10	10	1.25	15	317	0.139	89.43
11	10	12.5	1.25	20	325	0.131	98.87
12	10	12.5	1.5	25	585	0.158	93.16
13	10	15	1.25	15	471	0.159	88.57
14	10	10	1	20	398	0.154	90.19
15	10	12.5	1.5	15	512	0.165	87.51
16	10	10	1.25	25	468	0.178	91.64
17	10	12.5	1	25	729	0.214	92.21

Footnote: Batch 11 represents an experimental Box-Behnken run; optimized formulation F11 discussed in the optimization section refers to the model-predicted optimum.

Preparation of Nanoemulsion

A high-speed homogenizer (JHG-54-P100, Shanghai Pulisheng Fusion Machinery Co., Ltd., China) was used to make the nanoemulsion [23]. To create a homogeneous oil phase, castor oil (10 mL) and liquid paraffin (15 mL) were combined with flucytosine in a clean, dry beaker. This mixed lipid system (10:15) was chosen for its complementary physicochemical properties: castor oil enhances drug solubilization and interfacial film formation. At the same time, liquid paraffin improves the stability of the hydrophobic core and reduces Ostwald ripening. In another beaker, S_{mix} consisting of Tween 80 and propylene glycol at a 1:1 ratio was prepared, selected based on preliminary

emulsification screening and pseudo-ternary phase diagram studies. Distilled water was added to the mixture, and the mixture was stirred until a homogeneous solution formed. The oil phase was then slowly added to the water phase (30:70 % v/v) with continuous stirring. Then the formed emulsion was agitated at 15000 rpm for 20 min. After that, the solution was sonicated (probe sonication) for 10 min to ensure that all ingredients were thoroughly mixed and that the nanoemulsion was formed [24,25].

CHARACTERIZATION OF NANOEMULSION

Particle size and Particle size distribution (PDI)

The size of the nanoemulsion particles was measured using the Zetasizer Ver 7.13 (Malvern Instruments, Ltd, UK) in three separate measurements. An aliquot of approximately 1 mL was extracted and transferred into a cuvette. The mean particle diameter and polydispersity index (PDI) were determined at a temperature of 25±2ºC using a light scattering angle of 90º. The polydispersity index (PDI) was used to assess the distribution and uniformity of the globules. A PDI value less than 0.3 was deemed indicative of monodispersity [26].

Zeta potential

Zeta potential measurements were used to determine the strength of repulsion and attraction between nanoemulsion globules by detecting the electric charges on their surfaces [27]. A Malvern Zetasizer (Malvern Instruments, Worcestershire, UK) was used to evaluate the zeta potential of every formulation. The sample was diluted with distilled water from 50 µl up to 10 mL, and the measurement was carried out at a temp. of 25±2ºC.

Morphology study by transmission electron microscopy (TEM)

The nanoemulsion's morphology was examined via transmission electron microscopy (TEM), an essential method for confirming particle size and structural attributes. A minimal amount of the nanoemulsion was first placed on wax paper and then transferred to a circular copper grid (300-mesh). The specimen was stained with a 2% w/v phosphotungstic acid solution, air-dried under ambient circumstances, and subsequently analyzed using a Morgagni 268D transmission electron microscope (FEI, USA) at an accelerating voltage of 70 kV [28].

pH and conductivity measurement

The pH of the nanoemulsion formulations was measured with a digital pH meter (EUTECH Instruments, Singapore) at a controlled temperature of 25±2ºC, with triplicate measurements to ensure precision. Electrical conductivity was assessed by passing an electric current through a 20 mL sample at the same temperature using a conductivity meter (Model No. DB-1038, Decibel, India) fitted with Pt/platinised electrodes to evaluate formulation characteristics and phase behavior [29].

% Entrapment efficiency (% EE)

The entrapment efficiency of flucytosine nanoemulsion was quantitatively assessed by measuring the amount of unbound flucytosine in the dispersed aqueous phase. Briefly, a 2 mL sample of flucytosine nanoemulsion dispersion was centrifuged in an Eppendorf tube for 20 min at 12000 rpm using a cooling centrifuge manufactured by REMI Instruments Ltd., India. The centrifugation was carried out at 4 °C. After appropriate dilution with methanol, the supernatant was filtered. Flucytosine was then quantified using UV spectroscopy at a wavelength of 285 nm [30]. The %EE was determined using the following equation-

$$\%EE = \frac{\textbf{Totel quantity of flucytosine} - \textbf{Free quantity of flucytosine in supernatant}}{\textbf{Total quantity of flucytosine}} \times 100$$

RESULTS

Pre-formulation studies

Solubility Study

The solubility of flucytosine was evaluated in various formulation components to identify suitable excipients. Among the tested oils, castor oil exhibited a higher solubilization capacity than liquid paraffin. Tween 80 showed excellent solubilizing and emulsifying ability among surfactants, while propylene glycol demonstrated good solubility enhancement as a cosurfactant. Based on these findings, castor oil, Tween 80 & propylene glycol were selected for nanoemulsion formulation.

UV-visible spectroscopy

Absorption maxima (λ_{max}) of flucytosine were determined in 0.1N HCl. It was found to be 285 nm, as shown in Figure 1A.

Fourier Transform Infra-Red Spectroscopy (FTIR)

The FTIR spectrum of Flucytosine showed distinctive absorption bands that matched its functional groups, verifying the compound's identity. The main amino group's ($–NH_2$) N–H stretching vibration is responsible for a wide absorption band seen in the 3400–3200 cm^{-1} range. The pyrimidinone carbonyl group's C=O stretching vibration is responsible for the significant absorption at 1700–1650 cm^{-1}. Bands in the 1620–1550 cm^{-1} range are attributed to the pyrimidine ring's C=N

stretching and N–H bending vibrations. The heterocyclic ring's skeletal vibrations and C–N stretching are linked to the peaks between 1500 and 1200 cm^{-1}. Additionally, the presence of the fluorine substituent is confirmed by the absorption bands in the 1150–1000 cm^{-1} and 700–500 cm^{-1} area, which are typical of C–F stretching and bending vibrations. Substituted pyrimidine compounds typically exhibit ring deformation and out-of-plane bending vibrations, which are represented by multiple separate peaks in the fingerprint area below 1000 cm^{-1}.

Overall, the reported spectral properties of flucytosine and the observed FTIR spectrum coincide well, demonstrating the sample's purity and structural integrity as well as the existence of the anticipated functional groups (Table 3 and Figure 1B).

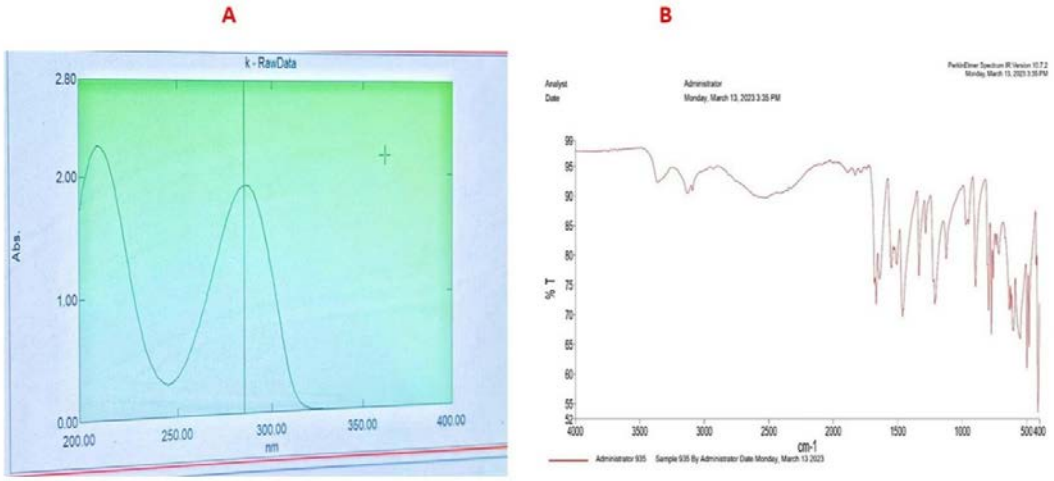

Figure 1: A. UV Spectrum of flucytosine. B. FTIR Spectrum of flucytosine

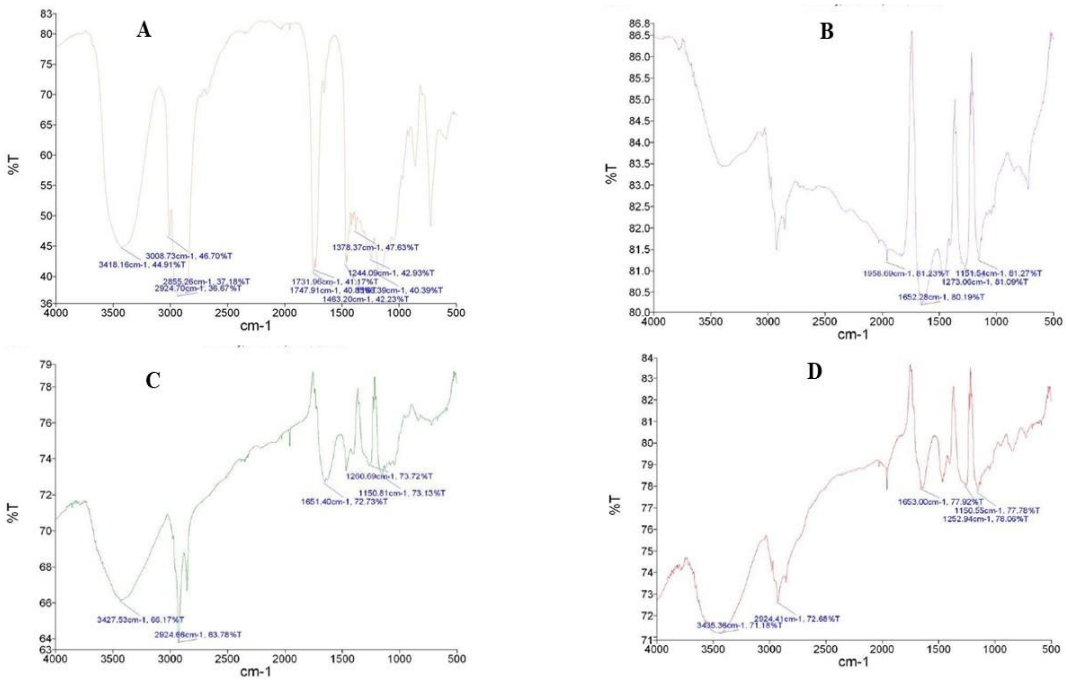

Figure 2: FTIR spectrum: A. Liquid Paraffin with drug, B. Castor Oil with drug, C. Propylene glycol 400 with drug and D. Tween 80 with drug

Drug-excipient compatibility studies

The FTIR spectra (Figure 2 and Table 3) demonstrate the presence of the distinctive peaks of flucytosine in all four combinations, with some shifts, suggesting the absence of any potential interactions. Nevertheless, no further peaks or notable alterations were detected, indicating that flucytosine is compatible with castor oil, liquid paraffin, propylene glycol, and Tween 80. The observed alterations in excipient-drug interactions are within acceptable limits, suggesting no

significant chemical incompatibilities between flucytosine and the excipients studied.

X-ray diffraction (XRD) study

The X-ray diffraction (XRD) pattern of flucytosine, seen in Figure 3, ranges from 0 to 80º on the 2θ axis. The count-based intensity of diffraction peaks is plotted as a function of 2θ. The prominent peaks detected in the pattern occur at around 10º, 12º, 15º, 20º, 22º, and 26º. The peak with the highest strength reaches approximately 1500 counts, indicating a significant diffraction signal at that particular angle. The distinct, well-defined peaks indicate that the flucytosine sample is in a crystalline state.

Table 3: Major peaks observed in the FTIR Spectrum in drug excipient compatibility studies

S. No.	Groups	Reported peak (cm^{-1})	Observed peak (cm^{-1})
1	NH stretching	3350	3418.16
2	CH stretching	3040	3088.73
3	C=C stretching	1675	1653.28
4	C=O stretching	1725	1731.69
5	C-H bending	1482	1458.45
6	C-N	1270	1270.10

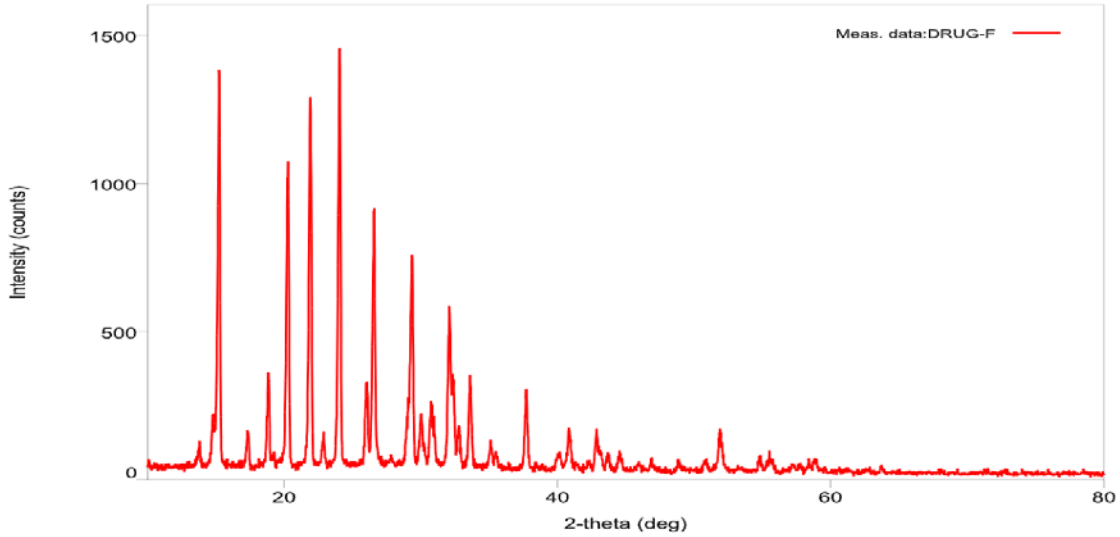

Figure 3: XRD spectrum of flucytosine

FORMULATION DEVELOPMENT

Experimental Design for the Formulation of Nanoemulsion

Nanoemulsion containing flucytosine was prepared using the high-speed homogenizer (8000-30000 rpm) and optimized using the BBD approach [31,32]. The research indicated that essential independent variables—specifically lipid concentration, Smix ratio, and homogenization duration—substantially affected key response measures, including particle size, polydispersity index (PDI), and entrapment efficiency. Principles of experimental design were methodically applied, encompassing hypothesis formulation, control of variability, and the judicious selection of variables and conditions. The observed responses were analyzed using first-order, second-order, and quadratic models, with the quadratic model demonstrating the optimal fit for all parameters. The elevated coefficients of determination (R^2) for particle size (0.9965), PDI (0.9866), and entrapment efficiency (0.9770) validated the model's resilience and predictive accuracy. The ANOVA findings, including sums of squares, degrees of freedom, mean squares, F-values, and p-values for each model term, are presented in Tables 5–7. Moreover, analysis of variance (ANOVA) confirmed the statistical significance of the models ($p < 0.05$), with elevated F-values demonstrating the substantial impact of formulation factors on the responses. The non-significant lack-of-fit values ($p > 0.05$) further validated the models' ability to depict the experimental data accurately.

Effect of formulation variables on particle size

The particle size of the prepared flucytosine-loaded nanoemulsion [33] is shown in Table 2. Table 2 shows that all nanoemulsion formulations had small particle sizes. The response surface and cube plots in Figure 4A illustrate how the flucytosine concentration in the quantity of lipid (X1), S_{mix} (X2), and homogenization time (X3) affects the particle size. The two-factor interaction model was statistically significant and accurately represented the observed particle size data, as shown by the ANOVA results. The following equation was produced using coded values:

$$\boldsymbol{Particle\ size} = \mathbf{2827.68} + \mathbf{246.5}(\boldsymbol{X_1}) - \mathbf{4152.5}(\boldsymbol{X_2}) - \mathbf{154.945}(\boldsymbol{X_3}) - \mathbf{57.6}(\boldsymbol{X_1})(\boldsymbol{X_2}) - \mathbf{2.12}(\boldsymbol{X_1})(\boldsymbol{X_3}) - \mathbf{19}(\boldsymbol{X_2})(\boldsymbol{X_3}) - \mathbf{4.428}(\boldsymbol{X_1})^2 + \mathbf{2017.2}(\boldsymbol{X_2})^2 + \mathbf{5.403}(\boldsymbol{X_3})^2 - - - (\mathbf{2})$$

The sign of the coefficient determines whether a factor has an increasing or decreasing effect on the nanoemulsion's particle-size range. Positive (+) values (e.g., +246.5(X1), +2017.2(X2)²) indicate that an increase in the corresponding variable results in an increase in particle size. Conversely, negative (-) values (e.g., -4152.5(X2), -154.945(X3)) indicate that an increase in the corresponding variable leads to a decrease in particle size. The statistical significance of the model and its terms is further supported by the ANOVA results presented in Table 4.

Effect of formulation variables on Polydispersity index (PDI)

The polydispersity index of the nanoemulsion loaded with flucytosine that was synthesized is indicated in Table 2. Table 2 shows that every nanoemulsion formulation had a low polydispersity index (PDI). The effects of flucytosine concentration (X1), Smix (X2), and homogenization time (X3) on PDI are illustrated by the response surface and cube plots in Figure 4 B. The two-factor interaction model was statistically significant and accurately represented the observed PDI data, as indicated by the ANOVA results [34]. The following was the final equation in terms of coded values:-

$$\boldsymbol{PDI} = \mathbf{0.566875} - \mathbf{0.02925}(\boldsymbol{X_1}) - \mathbf{0.033}(\boldsymbol{X_2}) - \mathbf{0.026475}(\boldsymbol{X_3}) + \mathbf{0.0128}(\boldsymbol{X_1})(\boldsymbol{X_2}) - \mathbf{0.000020}(\boldsymbol{X_1})(\boldsymbol{X_3}) - \mathbf{0.0168}(\boldsymbol{X_2})(\boldsymbol{X_3}) + \mathbf{0.00066}(\boldsymbol{X_1})^2 + \mathbf{0.07}(\boldsymbol{X_2})^2 + \mathbf{0.001285}(\boldsymbol{X_3})^2 - - - -(\mathbf{3})$$

This equation indicates that positive (+) values (e.g., +0.0128(X1)(X2), +0.07(X2)², +0.001285(X3)²) signify that an increase in the corresponding variable leads to an increase in the polydispersity index (PDI). Conversely, negative (-) values (e.g., -0.02925(X1), -0.033(X2), -0.026475(X3), -0.0168(X2)(X3)) indicate that an increase in the corresponding variables results in a decrease in PDI. The ANOVA results for the PDI model are summarized in Table 6.

Effect of Formulation Variables on Percent Entrapment Efficiency (%EE)

Table 2 shows the percentage EE of the prepared flucytosine-loaded nanoemulsion. Every nanoemulsion formulation showed a high %EE (Table 2). Figure 4C shows the cube plots and response surface for the effects of homogenization time (X3), Smix (X2), and flucytosine concentration on the lipid amount (X1) on the percentage entrapment efficiency (%EE). The results of the ANOVA test demonstrate that the two-factor interaction model was both significant and well-fitting to the observed PDI data. In terms of coded values, the resulting equation was as follows:

$$\%\,\boldsymbol{EE} = \mathbf{134.203} + \mathbf{13.687}(\boldsymbol{X_1}) + \mathbf{146.06}(\boldsymbol{X_2}) + \mathbf{5.1169}(\boldsymbol{X_3}) - \mathbf{1.956}(\boldsymbol{X_1})(\boldsymbol{X_2}) + \mathbf{0.0606}(\boldsymbol{X_1})(\boldsymbol{X_3}) + \mathbf{0.578}(\boldsymbol{X_2})(\boldsymbol{X_3}) - \mathbf{0.49284}(\boldsymbol{X_1})^2 - \mathbf{53.764}(\boldsymbol{X_2})^2 - \mathbf{0.15501}(\boldsymbol{X_3})^2 - - - -(\mathbf{4})$$

This equation demonstrates that positive (+) values (e.g., +13.687(X1), +146.06(X2), +5.1169(X3), +0.0606(X1)(X3), +0.578(X2)(X3)) contribute to an increase in % EE as the corresponding variables increase. In contrast, negative (-) values (e.g., -1.956(X1)(X2), -0.49284(X1)², -53.764(X2)², -0.15501(X3)²) indicate that an increase in the respective variables results in a decrease in %EE. This highlights the factors, i.e., homogenization time, Smix, and lipid amount, that significantly influence encapsulation efficiency. The ANOVA results confirming model significance for %EE are shown in Table 7.

Formulation optimization and analysis of the Box-Behnken design (BBD)

The experimental trials were methodically structured and evaluated using the Box–Behnken design (BBD), which requires fewer experimental runs than a full-factorial design while still delivering dependable optimization results. The model's adequacy and precision were assessed using the signal-to-noise ratio, with all responses exceeding 4, indicating an appropriate degree of model reliability. Additionally, the anticipated R^2 values were computed to assess the model's predictive performance, and their close alignment with the adjusted R^2 values (within ±0.20) validated the model's robustness and validity [35].

An optimized formulation with an overall desirability of 0.754 was established using Design-Expert software by imposing limits on particle size, polydispersity index (PDI), and entrapment efficiency. The optimized formulation parameters were a homogenization duration of 20.85 minutes, a lipid concentration of 10.95% v/v, and a Smix ratio of 1.205. This formulation was empirically developed and verified. Batch 11 served as an experimental run with a particle size of 325 nm and a PDI of 0.131. In contrast, the optimized formulation (F11), as predicted by the desirability function, exhibited enhanced properties with a particle size of 318.18 nm and a PDI of 0.136, thereby validating the optimization strategy.

CHARACTERIZATION OF NANOEMULSION

Globule size and Particle size distribution [36]

A narrow, consistent distribution of the nanoemulsions was confirmed by DLS particle-size distribution analysis (Figure 5B). The formulated preparations demonstrated particle sizes between 317 & 729 nm, with PDI values ranging from 0.118 to 0.214. The optimized formulation (F11) exhibited a particle size of 318.18 nm and a low PDI of 0.136, indicating a homogeneous, monodisperse system suitable for topical application.

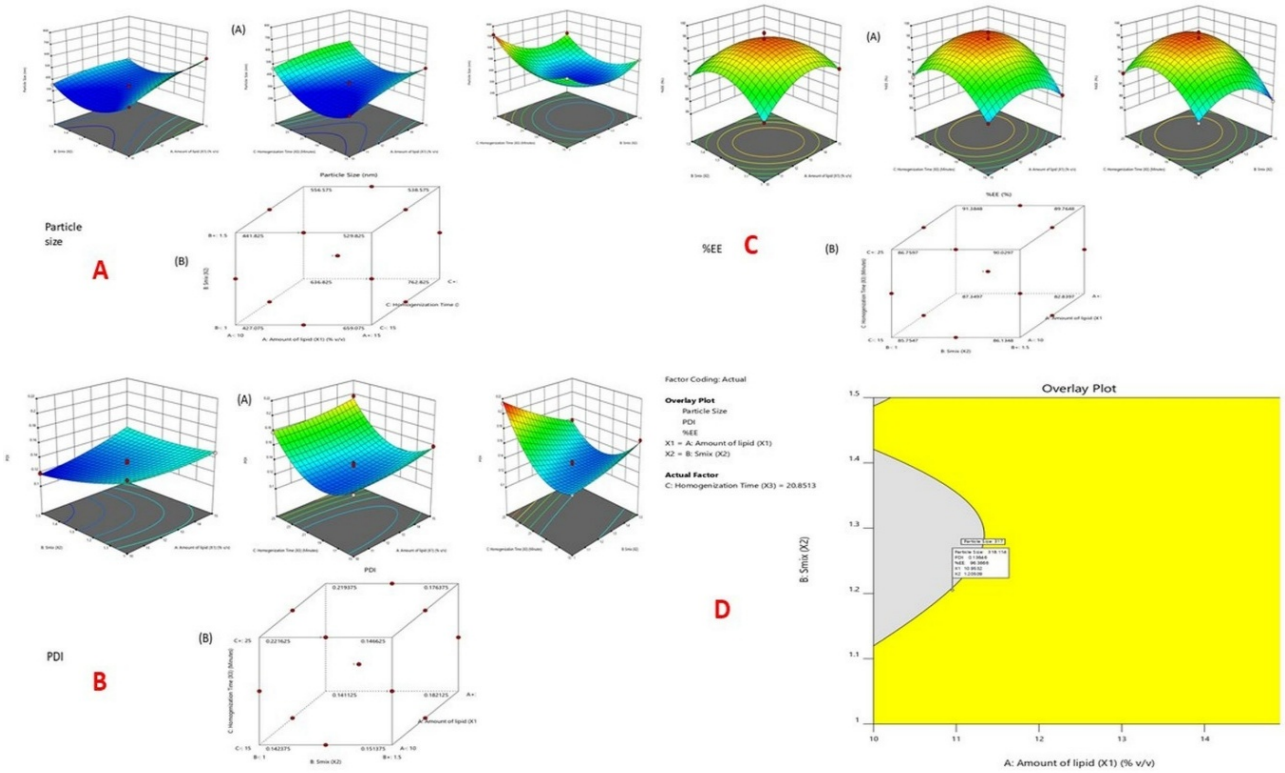

Figure 4: Response surface plots and cube plots illustrating the effect of lipid concentration (X1), S_{mix} (X2), and homogenization time (X3) on (A) particle size, (B) polydispersity index, (C) entrapment efficiency, and (D) overlay plot showing optimized formulation region

Table 4: Results of regression analysis for responses Y1 (Particle size), Y2 (PDI) and Y3 (%EE).

Response	Model	Adequate precision	R^2	Adjusted R^2	Predicted R^2	SD	%CV	p-values
Y1 (PS)	Quadratic	50.97	0.9965	0.9921	0.9659	10.72	2.41	<0.001
Y2 (PDI)	Quadratic	28.88	0.9866	0.9693	0.8701	0.0045	2.97	<0.001
Y3(%EE)	Quadratic	15.83	0.9770	0.9474	0.9543	0.84	0.90	<0.001

Table 5: ANOVA for Particle Size (Y1)

Source	Sum of Squares	df	Mean Square	F-value	p-value	
Model	2.314E+05	9	25712.64	223.74	< 0.0001	significant
A-Amount of lipid (X1)	22898.00	1	22898.00	199.25	< 0.0001	
B-Smix (X2)	21945.12	1	21945.12	190.96	< 0.0001	
C-Homogenization Time (X3)	23871.13	1	23871.13	207.72	< 0.0001	
AB	5184.00	1	5184.00	45.11	0.0003	
AC	2809.00	1	2809.00	24.44	0.0017	
BC	2256.25	1	2256.25	19.63	0.0030	
A^2	3224.87	1	3224.87	28.06	0.0011	
B^2	66925.92	1	66925.92	582.36	< 0.0001	
C^2	76822.13	1	76822.13	668.48	< 0.0001	
Residual	804.45	7	114.92			
Lack of Fit	461.25	3	153.75	1.79	0.2880	not significant
Pure Error	343.20	4	85.80			

Table 6: ANOVA for PDI (Y2)

Source	Sum of Squares	df	Mean Square	F-value	p-value	
Model	0.0104	9	0.0012	57.08	< 0.0001	significant
A-Amount of lipid (X1)	0.0004	1	0.0004	20.13	0.0028	
B-Smix (X2)	0.0006	1	0.0006	28.64	0.0011	
C-Homogenization Time (X3)	0.0027	1	0.0027	133.86	< 0.0001	
AB	0.0003	1	0.0003	12.69	0.0092	
AC	2.500E-07	1	2.500E-07	0.0124	0.9145	
BC	0.0018	1	0.0018	87.42	< 0.0001	
A^2	0.0001	1	0.0001	3.55	0.1015	
B^2	0.0001	1	0.0001	3.99	0.0858	
C^2	0.0043	1	0.0043	215.34	< 0.0001	
Residual	0.0001	7	0.0000			
Lack of Fit	0.0001	3	0.0000	1.70	0.3030	not significant
Pure Error	0.0001	4	0.0000			

Table 7: ANOVA for %EE (Y3)

Source	Sum of Squares	df	Mean Square	F-value	p-value	
Model	211.68	9	23.52	33.01	< 0.0001	significant
A-Amount of lipid (X1)	0.8845	1	0.8845	1.24	0.3020	
B-Smix (X2)	0.7688	1	0.7688	1.08	0.3334	
C-Homogenization Time (X3)	31.44	1	31.44	44.13	0.0003	
AB	5.98	1	5.98	8.39	0.0231	
AC	2.30	1	2.30	3.22	0.1157	
BC	2.09	1	2.09	2.93	0.1306	
A^2	39.95	1	39.95	56.07	0.0001	
B^2	47.54	1	47.54	66.73	< 0.0001	
C^2	63.23	1	63.23	88.75	< 0.0001	
Residual	4.99	7	0.7124			
Lack of Fit	0.1466	3	0.0489	0.0404	0.9876	not significant
Pure Error	4.84	4	1.21			

Zeta Potential

Figure 5C demonstrates that the optimized flucytosine nanoemulsion displayed a zeta potential of -22.2 mV, signifying moderate electrostatic stabilization. While zeta potential values exceeding ±30 mV are often associated with highly electrostatically stabilized dispersions, this nanoemulsion system achieves kinetic stability through a synergistic electrostatic and steric stabilization mechanism. The negative surface charge, presumably originating from free fatty acid residues in the lipid phase, induces repulsive interactions between droplets. In contrast, the non-ionic surfactant/co-surfactant system (Tween80 & propylene glycol) provides steric hindrance that mitigates droplet aggregation and coalescence. Moreover, the low PDI (0.136) & homogeneous nanosized droplet distribution indicate excellent colloidal stability. The measured zeta potential of -22.2 mV was deemed adequate to provide long-term kinetic stability in this particular surfactant-stabilized nanoemulsion system.

pH and conductivity measurement

At 25±2°C, the pH of the nanoemulsion formulation was determined. Within the typical pH range (5 to 6.5) of human skin, the nanoemulsion that was produced maintained a consistent pH of 6.10±0.16. This suggests that the nanoemulsion is non-irritating. This confirms that the formulation is O/W-type, as the optimized flucytosine nanoemulsion exhibited a conductivity of 249.48±2.14 μS/cm.

Morphology study by TEM

The optimized flucytosine nanoemulsion TEM (Figure 5A) showed mostly spherical and distinct globules with smooth surfaces and uniform distribution. Surfactants stabilized nanoemulsion droplets, which were well dispersed and did not aggregate. Most globules were nanometric, consistent with DLS particle-size analysis. The optimized formulation's homogeneity and stability were confirmed by its consistent shape and restricted size distribution.

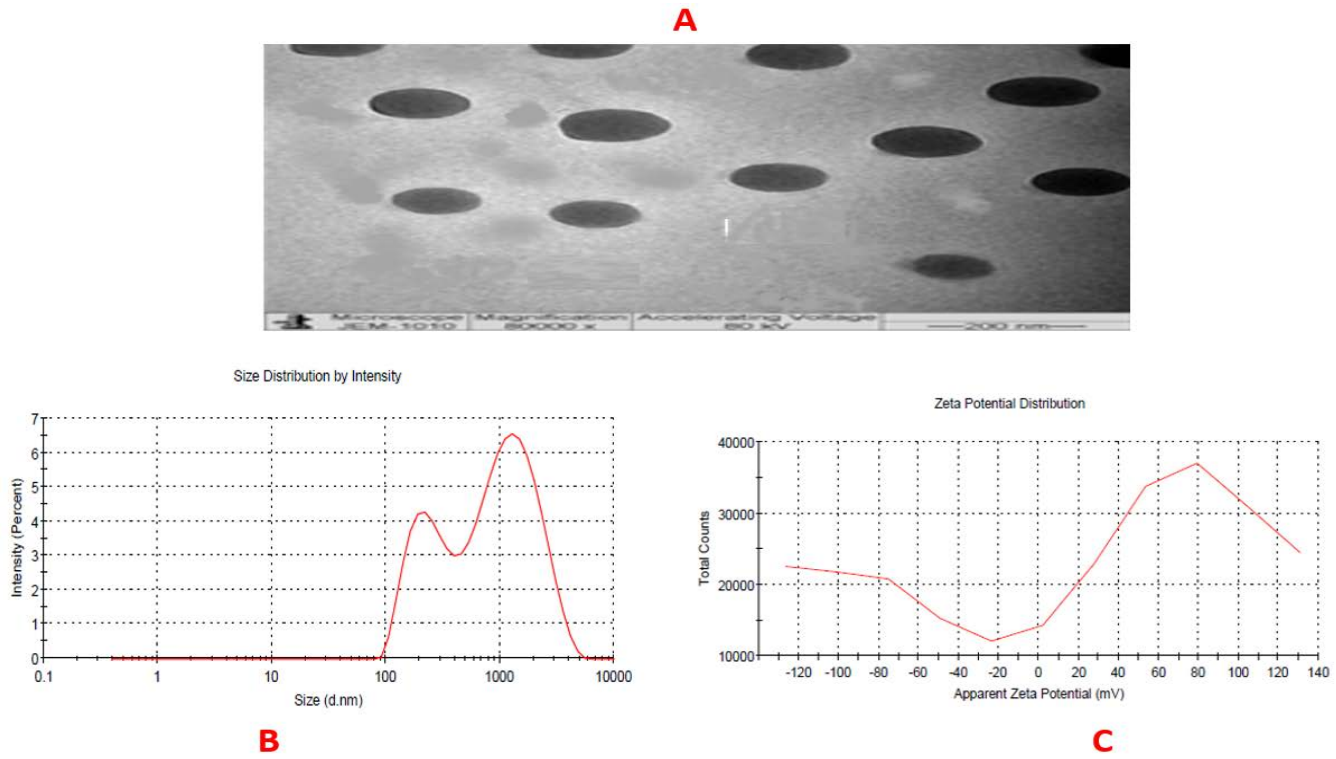

Figure 5: (A) TEM image of optimized flucytosine nanoemulsion (F11) showing spherical morphology; (B) Particle size distribution obtained by Dynamic Light Scattering (DLS); (C) Zeta potential of optimized nanoemulsion

% Entrapment efficiency (%EE)

The %EE of prepared flucytosine nanoemulsions (F1-F17) was found to be in the range of 87.51-98.89% (Table 2). Based on the results, flucytosine nanoemulsion (F11) was optimized with % EE (96.36%).

DISCUSSION

PRE-FORMULATION STUDIES

Solubility Study

Solubility screening is a critical step in nanoemulsion development, as it directly influences drug loading and formulation stability. In this study, castor oil demonstrated superior solubilization of flucytosine, which may be attributed to its long-chain fatty acid composition. Tween 80, due to its high HLB value, facilitated the formation of a stable oil-in-water nanoemulsion by reducing interfacial tension. Propylene glycol enhanced drug solubility and improved interfacial flexibility, promoting better dispersion of the oil phase. The selection of these excipients ensured efficient drug incorporation and contributed to the stability and performance of the optimized nanoemulsion.

UV-Visible Spectroscopy

The UV spectroscopy graph provides vital insights into the absorption spectrum of flucytosine. The distinct peaks observed at a particular wavelength (285 nm) aid in the identification & quantification of flucytosine in a given sample.

Fourier Transform Infra-Red Spectroscopy(FTIR)

The FTIR spectrum of flucytosine exhibits distinct peaks that correlate to its functional groups, such as N-H stretching, aromatic C-H stretching, aliphatic C-H stretching, C=O stretching, C=C stretching, N-H bending, C-H bending, N-O stretching, C-N stretching, and C-O stretching. These combined peaks confirm the presence of the relevant functional groups and the structural integrity of flucytosine. The fingerprint region further provides unique vibrational modes that can be used for identification and to confirm purity [37].

Drug Compatibility Study

We used FTIR spectra to demonstrate the presence of the distinctive peaks of flucytosine in all four combinations, with some shifts, suggesting the absence of any potential interactions. Nevertheless, no further peaks or notable alterations were detected, indicating that flucytosine is compatible with castor oil, liquid paraffin, propylene glycol, and Tween 80. The observed alterations in excipient-drug interactions are within acceptable limits, suggesting no significant chemical incompatibilities between flucytosine and the excipients studied.

X-ray diffraction (XRD) study

The XRD pattern of flucytosine confirms its crystalline structure, with distinct peaks at specific 2θ angles indicating diffraction from specific crystallographic planes within the sample. The high-intensity peaks suggest a high concentration of atoms or favorable diffraction orientation. The most prominent peaks at 10°, 12°, 15°, 20°, 22°, and 26° indicate well-defined crystallographic planes. The highest peak, at nearly 1500 counts, indicates a significant crystallographic plane under optimal diffraction conditions. The XRD analysis confirms the crystalline state of flucytosine, showcasing the ordered atomic arrangement within the sample. This crystallinity is crucial for understanding the material's physical properties, which can impact its performance and stability in pharmaceutical formulations. The data is critical for further applications and characterization in the development of pharmaceutical products.

FORMULATION DEVELOPMENT

Excipients Justification

The rational selection of excipients based on solubility and emulsification behavior plays a significant role in nanoemulsion formulation. The combination of castor oil, Tween 80, and propylene glycol provided an optimal balance between drug solubilization, emulsification efficiency, and stability. Similar excipient systems have been widely reported in the literature for enhancing drug bioavailability via nanoemulsions, supporting the suitability of the selected components in this study.

Experimental Design for the Formulation of Nanoemulsion

The Box-Behnken Design (BBD) methodology was employed to optimize and characterize a flucytosine-loaded nanoemulsion. The objective of the study was to assess the influence of three separate factors, namely lipid quantity, S_{mix}, and homogenization duration, on important quality characteristics such as particle size, polydispersity index (PDI), and entrapment efficiency. The BBD tool detected significant correlations between the independent and dependent variables, indicating that changes in these variables led to substantial alterations in particle size, PDI, and entrapment efficiency. The quadratic model yielded the most accurate fit for all response parameters, suggesting intricate interplay among variables. The high R^2 values for particle size, PDI, and entrapment efficiency confirm the model's predictive power and accuracy. The results indicate that precise manipulation of these factors can effectively regulate the characteristics of the flucytosine nanoemulsion, yielding a nanoemulsion with the required particle size and uniform distribution. This approach also maximizes the amount of drug trapped in the nanoemulsion, thereby improving its therapeutic effectiveness. This study emphasizes the importance of optimization techniques in nanoemulsion formulation and highlights their potential for medication delivery systems.

Effect of formulation variables on particle size

The coefficient of the term X1 signifies the extent to which the lipid content has a synergistic impact on the particle size of the manufactured nanoemulsion (p<0.0001) [38]. Optimal lipid concentrations facilitate the formation of smaller particles, while excessively high lipid concentrations result in larger particle sizes. This is probably due to greater thickness and the tendency of lipid molecules to form clusters [39]. The second-order coefficient, X2, also demonstrated the synergistic impact of S_{mix} on the particle size (p<0.0001) [40]. The presence of sufficient surfactant ensures effective emulsification and stabilization of lipid particles, thereby reducing particle size. Inadequate emulsification due to insufficient surfactant results in the formation of larger particles. The coefficient of the third term, X3, indicates that homogenization duration has a synergistic effect on the synthesized nanoemulsion's particle size (p<0.0001) [41]. Proper homogenization ensures complete blending and efficient reduction in lipid particle size. Extended homogenization durations typically reduce particle size, likely because the increased mechanical energy required to disintegrate particles is greater. The combined impact demonstrates that the smallest particle sizes are observed when the surfactant combination and homogenization duration are optimized, and the lipid quantity is kept at an appropriate lower level [42]. This demonstrates a synergistic phenomenon, in which each component amplifies the impact of the others. Optimal lipid quantity, surfactant combination, and homogenization duration are crucial for minimizing particle size and attaining consistent, small particles [43].

Effect of formulation variables on Polydispersity index (PDI)

The presence of a positive coefficient for the term X1 suggests that the lipid quantity has a synergistic impact on the polydispersity index (PDI) of the produced nanoemulsion. The observed effect is statistically significant, as indicated by a p-value of 0.0028. Increasing lipid concentration leads to a more consistent distribution of particle sizes (lower PDI), potentially because it forms a stronger framework that can efficiently contain and control particle size.

The second-term coefficient, X2, also demonstrated the combined effect of S_{mix} on the PDI (p=0.0011). The presence of an optimal amount of surfactant ensures effective emulsification and particle stabilization, thereby reducing polydispersity. Both insufficient and excessive quantities of surfactant can lead to elevated PDI. The third-order coefficient, X3, demonstrates that the duration of homogenization had a combined effect on the polydispersity index (PDI) of the resulting nanoemulsion (p<0.0001). Thorough homogenization ensures complete blending and reduces lipid droplet size, leading to a more uniform dispersion. The combined effect reveals that the lowest PDI values are observed when all three components are at their optimal higher levels. This demonstrates a synergistic phenomenon, in which each component amplifies the impact of the others. Optimal lipid quantity, surfactant composition, and homogenization duration are crucial for reducing PDI & attaining consistent particle sizes.

Effect of formulation variables on Percent Entrapment Efficiency (% EE)

The fact that the term X1 has a positive coefficient indicates that the lipid quantity enhances the entrapment effectiveness of the produced nanoemulsion (p<0.0001). There may be a correlation between the amount of lipid molecules available to form a stable matrix surrounding the payload and the enhanced encapsulation observed at higher lipid concentrations. S_{mix} improved entrapment efficiency synergistically, according to the ANOVA results [14]. The S_{mix} ratio plays a critical role in the formation and stability of nanoemulsion, which in turn affects entrapment efficiency. A balanced S_{mix} ratio reduces interfacial tension and promotes the formation of a stable interfacial film around the oil droplets. High surfactant concentrations can cause rigidity or micelle formation, reducing EE by increasing drug partitioning into the aqueous phase. Conversely, a higher cosurfactant proportion increases interfacial fluidity, allowing greater drug encapsulation. The optimal EE at a specific S_{mix} ratio is achieved by balancing interfacial tension reduction and film flexibility to promote efficient drug entrapment within the lipid core. The entrapment efficiency of the generated nanoemulsion was also synergistically influenced by the duration of homogenization, as indicated by the coefficient of the third term, X3 (p<0.0003). Proper homogenization ensures complete blending and reduces lipid droplet size, thereby enhancing encapsulation. The combined effect of these parameters indicates that the highest entrapment efficiency is achieved when all three factors are at their ideal maximum values. This exemplifies a synergistic phenomenon in which each component enhances the effects of the others. Maximizing the lipid quantity, surfactant composition, and homogenization duration is essential for achieving the highest achievable encapsulation efficiency.

Formulation optimization and analysis of the Box-Behnken (BB) design

The formulation of a nanoemulsion containing flucytosine, a highly effective antifungal agent, was optimized using the Box-Behnken design (BBD). Conventional oral antifungal treatments have limitations, and this study aimed to address fungal infections, such as blastomycosis and histoplasmosis, that don't respond to oral therapy due to poor absorption [44]. When treating these infections, the antifungal medicine flucytosine is essential, especially when used with amphotericin B. Particle size, polydispersity index, and percent entrapment efficiency were among the response metrics meticulously monitored during the optimization process, which also included tweaking formulation parameters. Small particle sizes, low polydispersity index (PDI), and high encapsulation efficiency (% EE) were desirable properties of the optimized nanoemulsion formulations. These properties have the potential to improve medication stability, absorption capacity, and targeted delivery. The formulation results were much influenced by the interaction between the S_{mix} ratio (X2) and lipid content (X1), as visualized in the overlay plot at a fixed homogenization time of 20.85 minutes (X3). Whereas the yellow area of the plot falls outside the optimal range, the grey area denotes the ideal formulation space that satisfies all desired criteria, as shown in Figure 4D. This work emphasizes how nanotechnology could improve drug delivery to address fungal infections.

CHARACTERIZATION OF NANOEMULSION

Particle size and Particle size distribution

Particle size plays a crucial role in delivering medications to the skin topically. Nano-sized droplets have a larger surface area, which promotes better drug absorption across membranes. This, in turn, increases drug release from the nanoemulsion, ultimately improving bioavailability. The optimized flucytosine nanoemulsion has a particle size of 318.18 nm. The small size improved absorption by increasing the surface area, thereby increasing the amount of flucytosine transported across the epidermal membrane. As a result, the therapeutic impact was enhanced, while the dosing frequency and the occurrence of

adverse effects were minimized. Furthermore, this size variety promoted even distribution due to reduced interfacial tension. PDI is commonly used to quantify the uniformity of droplet sizes in nanoemulsion. A smaller PDI value indicates a higher level of uniformity in the size of dispersed phase droplets, which in turn supports the superior stability of the emulsion [45]. The polydispersity index (PDI) ranges from 0.0 to 1.0, representing systems from monodisperse to highly polydisperse, with lower values indicating a uniform particle-size distribution and values near 1 indicating increased heterogeneity. A PDI value of 0.5 indicates a narrow size distribution, whereas higher values indicate greater diversity in droplet size. The optimized formulation in this investigation displayed a PDI of 0.136, indicating a uniform, homogeneous, and well-dispersed droplet system, hence confirming the stability & consistency of the nanoemulsion [46].

Zeta Potential

The zeta potential is a crucial characteristic affecting the stability of nanoemulsion systems, as it indicates the extent of electrostatic repulsion or attraction among dispersed droplets. An elevated zeta potential often improves stability by inhibiting droplet aggregation and coalescence, while diminished values may heighten the risk of instability [47]. A zeta potential of around ±30 mV is deemed adequate for ensuring electrostatic stabilization. This analysis revealed that the optimized nanoemulsion had a zeta potential of −22.2 mV, which, while slightly below the standard threshold, was sufficient to maintain stability. This results from the synergistic influence of modest electrostatic repulsion and robust steric stabilization conferred by the non-ionic surfactant (Tween 80). The droplets acquire a negative charge due to the presence of free fatty acids in the lipid phase. The low polydispersity index and homogeneous droplet size distribution enhance the system's kinetic stability, suggesting that the formulation is stable.

pH and conductivity measurement

The calculated pH of the nanoemulsion formulation was 25±2ºC. The stable pH values of the produced nanoemulsion were 6.10±0.18, falling within the typical range of human mucosa pH values (5 to 6.5), indicating that the nanoemulsion is non-irritating. To determine if an emulsion is water-in-oil (w/o) or o/w, the conductivity parameter is used. The conductivity of w/o type emulsions is lower than 1 µS/cm, but that of o/w type emulsions is higher [24,48]. When oil is the continuous phase in w/o emulsions, the formulation's conductivity is determined by its low conductivity relative to water, resulting in low values. The opposite is true for o/w emulsions. The optimized flucytosine nanoemulsion's conductivity of 249.48±2.14 µS/cm indicated that the formulation was O/W-type.

Morphology study by TEM

Transmission electron microscopy (TEM) confirmed that the optimized flucytosine nanoemulsion comprised primarily spherical, uniformly dispersed globules with smooth surface morphology. The droplets exhibited uniform dispersion and low aggregation, signifying effective steric stabilization conferred by Tween 80 and propylene glycol. The measured nanometric globule size aligned with DLS results; however, minor discrepancies between TEM and DLS measurements are anticipated, as DLS assesses hydrodynamic diameter in dispersion while TEM analyses dried particles. The consistent globular morphology and narrow particle-size distribution reinforce the stability and uniformity of the formulated nanoemulsion system, which are critical attributes for improved drug-delivery efficacy [49].

% Entrapment efficiency (%EE)

The study found that flucytosine nanoemulsions (F1-F17) exhibit high entrapment efficiency (%EE) ranging from 87.51% to 98.89%, indicating effective delivery of the active pharmaceutical ingredient. The flucytosine nanoemulsion (F11) was identified as the optimized formulation, achieving a %EE of 95%. This high entrapment efficiency is attributed to factors such as particle size, choice of surfactant and co-surfactant, and preparation method. The optimized formulation, F11, with a %EE of 96.36 %, is particularly promising for topical drug delivery applications. High entrapment efficiency ensures that a higher drug dose is available at the site of application, thereby enhancing the overall stability and efficacy of the nanoemulsion. This can lead to improved therapeutic outcomes, as a higher concentration of the active ingredient can penetrate the skin barrier and reach the target site more effectively [45]. The study successfully formulated a flucytosine nanoemulsion with high entrapment efficiency, demonstrating a promising approach to enhancing drug bioavailability and therapeutic efficacy.

CONCLUSION

This study successfully developed and optimized a flucytosine-loaded nanoemulsion using a Quality by Design approach based on the Box–Behnken design, demonstrating that formulation variables such as lipid concentration, Smix ratio, and

homogenization time significantly influence critical quality attributes. The optimized formulation (F11) exhibited advantageous physicochemical characteristics, including a particle size of 318.18 nm, a low polydispersity index of 0.136, a sufficient zeta potential of -22.2 mV, and a high entrapment efficiency of 96.36%, indicating stability, uniformity, and enhanced drug-loading capacity. Preformulation and compatibility studies confirmed the integrity and suitability of the drug-excipient system, while characterization results supported the nanoemulsion's potential for improved drug delivery efficacy.

The results highlight the effectiveness of statistical optimization in designing nanoemulsion systems that demonstrate enhanced bioavailability and therapeutic potential for antifungal therapy. The study is limited by the absence of in vivo evaluations, long-term stability assessments, and clinical validation, all of which are essential for thoroughly establishing the safety, efficacy, and translational significance of the product. Moreover, scalability and practical manufacturing factors were not assessed. In the current global context of increasing antifungal resistance and a rising incidence of invasive fungal infections, especially in immunocompromised patients, the development of advanced drug delivery technologies such as nanoemulsion is critically important. This study provides a potential basis for improving the therapeutic effectiveness of flucytosine and supports the further use of nanotechnology-based methods to address the limitations of conventional antifungal therapies.

The optimized flucytosine nanoemulsion exhibited favorable physicochemical characteristics and improved drug encapsulation, suggesting its potential as an efficient antifungal delivery system. Subsequent research should concentrate on *in vitro* drug release, *in vivo* assessment, long-term stability, and clinical translation to substantiate its therapeutic relevance. This method may enhance the management of resistant fungal diseases. The current study effectively optimized and characterized the flucytosine-loaded nanoemulsion; however, it is limited by the absence of in vitro drug-release studies. Such investigations are crucial for validating the drug release profile and corroborating improved delivery efficacy.

Future research will concentrate on assessing the in vitro release profile utilizing appropriate methodologies, including dialysis bag techniques. Subsequent research will assess antifungal efficacy against *Candida* and *Cryptococcus* and juxtapose the findings with those from pure flucytosine to validate the superior effectiveness of the nanoemulsion technology.

FINANCIAL ASSISTANCE
NIL

CONFLICT OF INTEREST
The authors declare no conflict of interest.

AUTHOR CONTRIBUTION
All authors made substantial contributions to conception and design, acquisition of data, or analysis and interpretation of data; took part in drafting the article or revising it critically for important intellectual content; agreed to submit to the current journal; gave final approval of the version to be published; and agree to be accountable for all aspects of the work.

DECLARATION OF USE OF AI TOOLS
The author used ChatGPT to check grammar and improve sentence clarity. All content, analysis, and conclusions were reviewed and verified by the authors. The authors take full responsibility for the originality, accuracy, and integrity of the work.

ABBREVIATIONS
DNA- Deoxyribonucleic Acid, **RNA-** Ribonucleic Acid, **BBD-** Box-Behnken Design, **PDI-** Polydispersity Index, **EE-** Entrapment Efficiency, **nm-** Nanometer, **mV-** Millivolt, **UV-** Ultraviolet, **FTIR-** Fourier transform infrared spectroscopy, **XRD-** X-ray diffraction, **5-FU-** 5-Fluorouracil, **NE-** Nanoemulsion, **HCl-** Hydrochloric Acid, **TEM-** Transmission Electron Microscopy, **ºC-** Degree Celsius

REFERENCES
[1] Lockhart SR, Chowdhary A, Gold JAW. The rapid emergence of antifungal-resistant human-pathogenic fungi. *Nat Rev Microbiol*, **21**, 818–832 (2023) https://doi.org/10.1038/s41579-023-00960-9
[2] Gorle A, Ahire K, Shende R. Design, development and characterization of nanoemulsion developed by high pressure homogenization (HPH) method containing antifungal drug. *J Drug Deliv Ther*, **12**, 24–32 (2022) https://doi.org/10.22270/jddt.v12i2.5245
[3] Sigera LSM, Denning DW. Flucytosine and its clinical usage. *Ther Adv Infect Dis*, **10**, 20499361231161388 (2023) https://doi.org/10.1177/20499361231161
[4] Miot J, Leong T, Takuva S, Parrish A, Dawood H. Cost-effectiveness analysis of flucytosine as induction therapy in the

treatment of cryptococcal meningitis in HIV-infected adults in South Africa. *BMC Health Serv Res*, **21**, 1–11 (2021) https://doi.org/10.1186/s12913-021-06268-9

[5] Sastré-Velásquez LE, Dallemulle A, Kühbacher A, Baldin C, Alcazar-Fuoli L, Niedrig A, et al. The fungal expel of 5-fluorocytosine derived fluoropyrimidines mitigates its antifungal activity and generates a cytotoxic environment. *PLoS Pathog*, **18**, e1011066 (2022) https://doi.org/10.1371/journal.ppat.1011066

[6] Salmanton-García J. Update on invasive fungal infections: emerging trends in the incidence of fungal infections in immunosuppressed patients and associated conditions. *Ther Adv Infect Dis*, **11** (2024) https://doi.org/10.1177/20499361241282835

[7] Iyer KR, Revie NM, Fu C, Robbins N, Cowen LE. Treatment strategies for cryptococcal infection: challenges, advances and future outlook. *Nat Rev Microbiol*, **19**, 454–466 (2021) https://doi.org/10.1038/s41579-021-00511-0

[8] Akkuş İ, Kaçmaz B. Antifungal drugs. *J Curr Hematol Oncol Res*, **1**, 41–46 (2023) https://doi.org/10.51271/JCHOR-0010

[9] Hilpert K, Rumancev C, Gani J, Collis DWP, Lopez-Perez PM, Garamus VM, et al. Can BioSAXS detect ultrastructural changes of antifungal compounds in Candida albicans? — an exploratory study. *Front Pharmacol*, **14**, 1141785 (2023) https://doi.org/10.3389/fphar.2023.1141785

[10] Shaker DS, Ishak RAH, Ghoneim A, Elhuoni MA. Nanoemulsion: a review on mechanisms for the transdermal delivery of hydrophobic and hydrophilic drugs. *Sci Pharm*, **87**, 17 (2019) https://doi.org/10.3390/scipharm87030017

[11] Nikolaev B, Yakovleva L, Fedorov V, Li H, Gao H, Shevtsov M. Nano- and microemulsions in biomedicine: from theory to practice. *Pharmaceutics*, **15**, 1989 (2023) https://doi.org/10.3390/pharmaceutics15071989

[12] Tayeb HH, Felimban R, Almaghrabi S, Hasaballah N. Nanoemulsion: formulation, characterization, biological fate, and potential role against COVID-19 and other viral outbreaks. *Colloid Interface Sci Commun*, **45**, 100533 (2021) https://doi.org/10.1016/j.colcom.2021.100533

[13] Rampado R, Peer D. Design of experiments in the optimization of nanoparticle-based drug delivery systems. *J Control Release*, **358**, 398–419 (2023) https://doi.org/10.1016/j.jconrel.2023.05.001

[14] Yadav P, Rastogi V, Verma A. Application of Box–Behnken design and desirability function in the development and optimization of self-nanoemulsifying drug delivery system for enhanced dissolution of ezetimibe. *Futur J Pharm Sci*, **6**, 1–20 (2020) https://doi.org/10.1186/s43094-020-00023-3

[15] Kamdi DB, Yerne HM, Patil SR. Development and validation of UV spectroscopic method for estimation of fluconazole in tablet dosage form. *Am J PharmTech Res*, **10**, 83–92 (2020) https://doi.org/10.46624/ajptr.2020.v10.i1.008

[16] Tkachenko Y, Niedzielski P. FTIR as a method for qualitative assessment of solid samples in geochemical research: a review. *Molecules*, **27**, 8846 (2022) https://doi.org/10.3390/molecules27248846

[17] Gupta M, Tiwari P. Formulation and in-vitro evaluation of oxaprozin transdermal patches for sustained anti-inflammatory therapy. *J Appl Pharm Res*, **13**, 22–32 (2025) https://doi.org/10.69857/joapr.v13i6.1203

[18] Ali A, Chiang YW, Santos RM. X-ray diffraction techniques for mineral characterization: a review for engineers of the fundamentals, applications, and research directions. *Minerals*, **12**, 205 (2022) https://doi.org/10.3390/min12020205

[19] Jufri M, Mun'im A, Zulfakar MH. Development and optimization of asiaticoside nanoemulsion formulation by Box-Behnken design. *Farmacia*, **72** (2024) https://doi.org/10.31925/farmacia.2024.6.19

[20] Chaturvedi S, Garg A. Development and optimization of nanoemulsion containing exemestane using Box-Behnken design. *J Drug Deliv Sci Technol*, **80**, 104151 (2023) https://doi.org/10.1016/j.jddst.2023.104151

[21] Mahapatra APK, Saraswat R, Botre M, Paul B, Prasad N. Application of response surface methodology (RSM) in statistical optimization and pharmaceutical characterization of a patient compliance effervescent tablet formulation of an antiepileptic drug levetiracetam. *Futur J Pharm Sci*, **6**, 1–14 (2020) https://doi.org/10.1186/s43094-020-00096-0

[22] Safhi AY, Naveen NR, Rolla KJ, Bhavani PD, Kurakula M, Hosny KM, et al. Enhancement of antifungal activity and transdermal delivery of 5-flucytosine via tailored spanlastic nanovesicles: statistical optimization, in-vitro characterization, and in-vivo biodistribution study. *Front Pharmacol*, **14**, 1321517 (2023) https://doi.org/10.3389/fphar.2023.1321517

[23] Shi Y, Zhang M, Chen K, Wang M. Nano-emulsion prepared by high pressure homogenization method as a good carrier for Sichuan pepper essential oil: preparation, stability, and bioactivity. *LWT*, **154**, 112779 (2022) https://doi.org/10.1016/j.lwt.2021.112779

[24] Jacob S, Kather FS, Boddu SHS, Shah J, Nair AB. Innovations in nanoemulsion technology: enhancing drug delivery for oral, parenteral, and ophthalmic applications. *Pharmaceutics*, **16**, 1333 (2024) https://doi.org/10.3390/pharmaceutics16101333

[25] Ahmad N, Ahmad R, Al-Qudaihi A, Alaseel SE, Fita IZ, Khalid MS, et al. Preparation of a novel curcumin nanoemulsion by ultrasonication and its comparative effects in wound healing and the treatment of inflammation. *RSC Adv*, **9**, 20192–20206 (2019) https://doi.org/10.1039/c9ra03102b

[26] Anwer MK, Aldawsari MF, Iqbal M, Almutairy BK, Soliman GA, Aboudzadeh MA. Diosmin-loaded nanoemulsion-based gel formulation: development, optimization, wound healing and anti-

inflammatory studies. *Gels*, **9**, 95 (2023) https://doi.org/10.3390/gels9020095

[27] Rasmussen MK, Pedersen JN, Marie R. Size and surface charge characterization of nanoparticles with a salt gradient. *Nat Commun*, **11**, 2337 (2020) https://doi.org/10.1038/s41467-020-15889-3

[28] Ahmad N, Ahmad R, Ahmad FJ, Ahmad W, Alam MA, Amir M, et al. Poloxamer-chitosan-based naringenin nanoformulation used in brain targeting for the treatment of cerebral ischemia. *Saudi J Biol Sci*, **27**, 500–517 (2020) https://doi.org/10.1016/j.sjbs.2019.11.008

[29] Farooq U, Rasul A, Zafarullah M, Abbas G, Rasool M, Ali F, et al. Nanoemulsion as novel nanocarriers for drug delivery across the skin: in-vitro, in-vivo evaluation of miconazole nanoemulsion for treatment of Candidiasis albicans. *Des Monomers Polym*, **24**, 240–258 (2021) https://doi.org/10.1080/15685551.2021.1965724

[30] Maharini I, Martien R, Nugroho AK, Supanji S, Adhyatmika A. Validation UV spectrophotometric method to determine entrapment efficiency of ocular polymeric nanoparticle levofloxacin hemihydrate. *Res J Pharm Technol*, **14**, 5479–5482 (2021) https://doi.org/10.52711/0974-360X.2021.00956

[31] Das T, Venkatesh MP, Kumar TMP, Koland M. SLN based alendronate in situ gel as an implantable drug delivery system — a full factorial design approach. *J Drug Deliv Sci Technol*, **55**, 101415 (2020) https://doi.org/10.1016/j.jddst.2019.101415

[32] Jain P, Taleuzzaman M, Kala C, Kumar Gupta D, Ali A, Aslam M. Quality by design (QbD) assisted development of phytosomal gel of aloe vera extract for topical delivery. *J Liposome Res*, **31**, 381–388 (2021) https://doi.org/10.1080/08982104.2020.1849279

[33] Gohil D, Shah N, Maheshwari RA. Effect of formulation variables on fabrication of risperidone loaded nanoparticles for sustained drug delivery. *Indian J Pharm Educ Res*, **56**, 58–64 (2022) https://doi.org/10.5530/ijper.56.1.8

[34] Gupta B, Poudel BK, Pathak S, Tak JW, Lee HH, Jeong JH, et al. Effects of formulation variables on the particle size and drug encapsulation of imatinib-loaded solid lipid nanoparticles. *AAPS PharmSciTech*, **17**, 652–662 (2016) https://doi.org/10.1208/s12249-015-0384-z

[35] Aggarapu S, Galla R, Shaik NJ, Dasari SJ. Application of Plackett–Burman and Box–Behnken designs to develop a sensitive and robust HPLC method for quantifying hypolipidemic drugs, rosuvastatin and bempedoic acid in tablets. *Futur J Pharm Sci*, **11**, 61 (2025) https://doi.org/10.1186/s43094-025-00814-6

[36] Kurakula M, Naveen NR, Patel B, Manne R, Patel DB. Preparation, optimization and evaluation of chitosan-based avanafil nanocomplex utilizing antioxidants for enhanced neuroprotective effect on PC12 cells. *Gels*, **7**, 96 (2021) https://doi.org/10.3390/gels7030096

[37] Parmar K, Bharatia R. Novel flucytosine loaded in-situ gel for the management of ocular infections. *Prospect Pharm Sci*, **23**, 75–83 (2025) https://doi.org/10.56782/pps.350

[38] Bakhaidar RB, Naveen NR, Basim P, Murshid SS, Kurakula M, Alamoudi AJ, et al. Response surface methodology (RSM) powered formulation development, optimization and evaluation of thiolated based mucoadhesive nanocrystals for local delivery of simvastatin. *Polymers (Basel)*, **14**, 5184 (2022) https://doi.org/10.3390/polym14235184

[39] Albertsen CH, Kulkarni JA, Witzigmann D, Lind M, Petersson K, Simonsen JB. The role of lipid components in lipid nanoparticles for vaccines and gene therapy. *Adv Drug Deliv Rev*, **188**, 114416 (2022) https://doi.org/10.1016/j.addr.2022.114416

[40] Algahtani MS, Ahmad MZ, Ahmad J. Investigation of factors influencing formation of nanoemulsion by spontaneous emulsification: impact on droplet size, polydispersity index, and stability. *Bioengineering*, **9**, 384 (2022) https://doi.org/10.3390/bioengineering9080384

[41] Alhakamy NA, Badr-Eldin SM, Ahmed OAA, Aldawsari HM, Okbazghi SZ, Alfaleh MA, et al. Green nanoemulsion stabilized by in situ self-assembled natural oil/native cyclodextrin complexes: an eco-friendly approach for enhancing anticancer activity of costunolide against lung cancer cells. *Pharmaceutics*, **14**, 227 (2022) https://doi.org/10.3390/pharmaceutics14020227

[42] Gawin-Mikołajewicz A, Nawrot U, Malec KH, Krajewska K, Nartowski KP, Karolewicz BL. The effect of high-pressure homogenization conditions on the physicochemical properties and stability of designed fluconazole-loaded ocular nanoemulsion. *Pharmaceutics*, **16**, 11 (2023) https://doi.org/10.3390/pharmaceutics16010011

[43] Khaleseh F, Barzegar-Jalali M, Zakeri-Milani P, Islambulchilar Z, Valizadeh H. Optimum surfactant concentration for preparation of amiodarone loaded solid lipid nanoparticles: theoretical estimation versus experimental results by Box-Behnken design. *J Rep Pharm Sci*, **12** (2023) https://doi.org/10.5812/jrps-146155

[44] Srivastava R, Rawat AKS. Formulation and evaluation of flucytosine-loaded nanoemulgel for enhanced antifungal activity through in vitro and in vivo studies. *J Appl Pharm Res*, **13**, 1–13 (2025) ⚠ *DOI not provided — please supply if available*

[45] Souto EB, Cano A, Martins-Gomes C, Coutinho TE, Zielińska A, Silva AM. Microemulsions and nanoemulsion in skin drug delivery. *Bioengineering*, **9**, 158 (2022) https://doi.org/10.3390/bioengineering9040158

[46] Yakoubi S, Kobayashi I, Uemura K, Nakajima M, Isoda H, Ksouri R, et al. Essential-oil-loaded nanoemulsion lipidic-phase optimization and modeling by response surface methodology (RSM): enhancement of their antimicrobial potential and bioavailability in nanoscale food delivery system. *Foods*, **10**, 3149 (2021) https://doi.org/10.3390/foods10123149

[47] Mohammed NK, Muhialdin BJ, Meor Hussin AS. Characterization of nanoemulsion of Nigella sativa oil and its application in ice cream. *Food Sci Nutr*, **8**, 2608–2618 (2020) https://doi.org/10.1002/fsn3.1500

[48] Preeti, Sambhakar S, Malik R, Bhatia S, Al Harrasi A, Rani C, et al. Nanoemulsion: an emerging novel technology for improving the bioavailability of drugs. *Scientifica (Cairo)*, **2023**, 6640103 (2023) https://doi.org/10.1155/2023/6640103

[49] Aldosari BN, Ibrahim MA, Alqahtani Y, El Sayeh AF. Formulation and evaluation of fluconazole nanosuspensions: in vitro characterization and transcorneal permeability studies. *Saudi Pharm J*, **32**, 102104 (2024) https://doi.org/10.1016/j.jsps.2024.102104